κ²*N*(imidazole), *S*(thioether) Macrochelation of [Pt(en)]²⁺ (en = H₂NCH₂CH₂NH₂) by terminal histidine and methionine side-chains in tri-, tetra- and penta-peptides

Dirk Wolters and William S. Sheldrick *

Lehrstuhl für Analytische Chemie, Ruhr-Universität Bochum, D-44780 Bochum, Germany.
E-mail: shel@anachem.ruhr-uni-bochum.de

The pH and time dependent reactions of [Pt(en)(H₂O)₂]²⁺ (en = H₂NCH₂CH₂NH₂) with the histidylmethionine peptides Hhis-gly-metH, Ac-his-gly-gly-metH [Ac = CH₃C(O)] and Ac-his-ala-ala-ala-metH (Hgly = glycine, Hala = L-alanine) at 313 K have been studied by ion-pairing reversed-phase HPLC and ¹H and ¹⁹⁵Pt NMR spectroscopy. Following initial anchoring of the [Pt(en)]²⁺ fragment on the thioether S in a κ²*O,S* complex, metallation of the neighbouring amide nitrogen is relatively rapid for all three peptides at pH < 4. After reaching a concentration maximum within 10–50 h, the resulting κ²*N*′met,*S* six-membered chelate slowly isomerizes to the thermodynamically preferred κ²*N*¹,*S* macrochelate and in the case of the tetra- and penta-peptides to the less favoured κ²*N*³,*S* complex as well. The speed of this reaction is significantly faster for the latter *i* + 4 spacing of the ligating residues, which brings the thioether S and imidazole donor atoms into close proximity for an α helix conformation. Although time dependent studies indicated that the macrochelates are formed at a comparable rate to the κ²*N*′met,*S* complexes in alkaline solution, a clear thermodynamic preference for the smaller methionine chelate is apparent for the longer peptides.

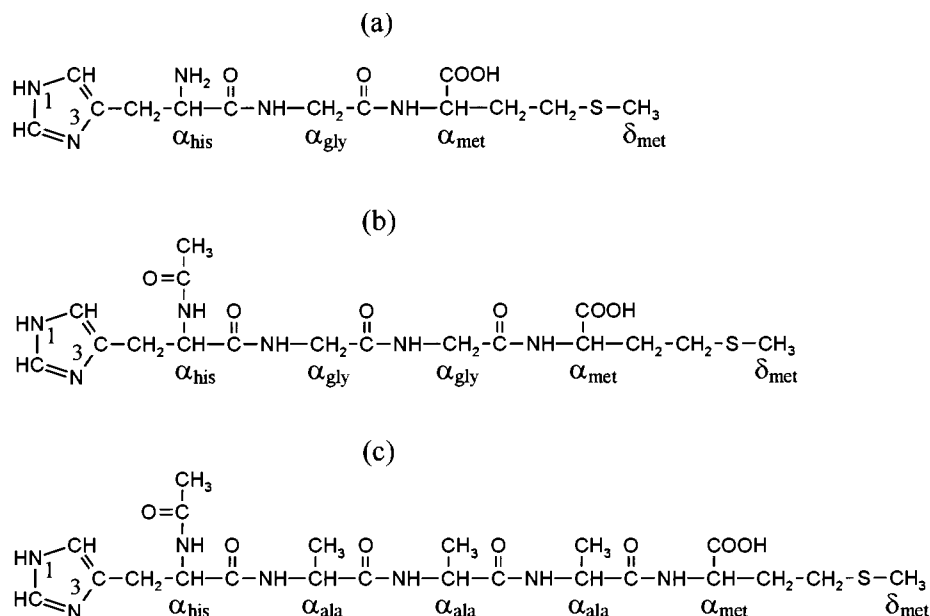The concentration-dependent nephrotoxicity of cisplatin, *cis*-[PtCl₂(NH₃)₂], and other platinum(II) anticancer drugs has been attributed to their pronounced kinetic affinity for sulfur-containing ligands such as the L-cysteine or L-methionine (Hmet) side chains of peptides and proteins.[1] One of the few fully characterized metabolites of cisplatin is indeed the bis-chelate [Pt(met-κ²*N,S*)₂], which has been isolated from the urine of chemotherapy patients.[2] Co-ordination through protein thioether sulfur ligands can take place as platinum(II) complexes pass through cell walls, leading to the formation of an intracellular drug reservoir composed of labile intermediates, that are then available for subsequent thermodynamically preferred DNA binding.[3] Support for such a platinum-pool mechanism has been provided by recent reports[4–7] of both inter- and intra-molecular replacement of a thioether S by a guanine N⁷ in the co-ordination sphere of the model fragment [Pt(dien)]²⁺ (dien = diethylenetriamine). For instance, the intramolecular migration of [Pt(dien)]²⁺ from the methionine residue of the nucleopeptide 5′-*O*-methioninate-*N*-ylcarbonylthymidine 2′-deoxyguanosine monophosphate Met-d(TpG) to the purine nucleobase is accomplished within 6 d at room temperature.[7] Contrastingly, treatment of Met-d(TpG) with bidentate [Pt(en)]²⁺ (en = ethane-1,2-diamine) affords a substitution inert κ²*S,N*⁷ macrochelate,[7] whose stability is in accordance with that of similar complexes.[8,9] Of considerable interest, in the context of a protein bound intracellular platinum(II) drug reservoir, is the observation that the rate of guanosine 5′-monophosphate binding by cisplatin increases in the presence of L-methionine, presumably owing to the labilization of an ammine ligand in the κ²*N,S* co-ordinated intermediate [Pt(met-κ²*N,S*)(NH₃)₂]⁺, as a result of the strong *trans* effect of the thioether sulfur.[10] Current interest in the platinum-pool mechanism has also prompted recent systematic studies on the reaction of [Pt(en)(H₂O)₂]²⁺, [Pt(en)(Me-mal-κ²*O,O*′)] (Me-mal = 2-methylmalonate) and [Pd(en)(H₂O)₂]²⁺ with methionine-containing peptides[11,12] and L-cysteine derivatives.[13]

Interestingly, whereas guanosine 5′-monophosphate select-ively displaces Hmet in [Pt(dien)(Hmet-κ*S*)]²⁺, no reaction is observed between the likewise imidazole-containing amino acid L-histidine (Hhis) and this complex, even after 3 d.[5] In contrast, our own HPLC and NMR investigations of the kinetics of competitive binding of monodentate [Pt(dien)]²⁺ by the neigh-bouring side chains in the dipeptide Hhis-metH revealed[14] that initial thioether S co-ordination at pH > 6 is indeed followed by slow migration of the metal fragment to an imidazole site, with N¹ being very clearly preferred over N³. A time-dependent study[15] of the reaction of [Pt(en)(H₂O)₂]²⁺ with the same dipeptide at pH 4.55 indicates that methionine S plays an anchoring role in directing further product formation following its initial rapid co-ordination. An intermediate κ²*O,S* chelate reaches its maximum concentration at 313 K after only 0.5 h and then slowly converts into two competitive S-bound com-plexes with respectively κ²*N*¹,*S* and κ²*N*′met,*S* co-ordination over a period of 5 h. The apparent preference of both [Pt(dien)]²⁺ and [Pt(en)]²⁺ for imidazole N¹ rather than N³ in Hhis-metH is in striking contrast to the 2:3 equilibrium ratio of linkage isomers established by Appleton *et al.*[16] for the reaction of the former monodentate metal fragment with Hhis itself.

A remarkable long-term kinetic stability over a period of 28 d was established[15] for [Pt(en)(Hhis-metH-κ²*N*¹,*S*)]²⁺ and this observation suggests that formation of κ²*N*¹,*S* (or κ*N*³,*S*) macrochelates by peptides or proteins could prevent the release of Pt^II for DNA binding from an intracellular drug reservoir and also possibly influence the metabolism of platinum anti-cancer drugs. With the goal of scrutinizing the more general applicability of this hypothesis to biological systems we have now extended our HPLC and NMR studies to the reaction of [Pt(en)(H₂O)₂]²⁺ with the longer peptides Hhis-gly-metH, Ac-his-gly-gly-metH [Ac = CH₃C(O)] and Ac-his-ala-ala-ala-metH (Hgly = glycine, Hala = L-alanine).

Our choice of Hhis-gly-metH (a), Ac-his-gly-gly-metH (b) and Ac-his-ala-ala-ala-metH (c) was governed both by the desire to study a sequence of small peptides with respectively

(a)

α_his   α_gly   α_met   δ_met

(b)

α_his   α_gly   α_gly   α_met   δ_met

(c)

α_his   α_ala   α_ala   α_ala   α_met   δ_met

(a) Hhis-gly-metH

(b) Ac-his-gly-gly-metH

(c) Ac-his-ala-ala-ala-metH

Fig. 1 Optimized conformations for the peptides (a) Hhis-gly-metH, (b) Ac-his-gly-gly-metH and (c) Ac-his-ala-ala-ala-metH on the basis of molecular modeling.[21]

one, two and three amino acid residues between competing histidine and methionine side chains and by recent reports on the stabilization of folded polypeptide chains by metal-mediated conformational restriction.[17,18] The typical α helix exhibits 3.6 residues per turn and peptides containing ligating side chains at i and $i + 4$ positions in their backbones have been observed to undergo a random coil to helix transition on macrochelation of an added divalent metal cation such as Cu^{2+}. Modeling considerations indicate that the geometric requirements for chelation will be fulfilled by dihistidyl sequences -his-x-his- in a β sheet, -his-x₂-his- in a reverse β turn and -his-x₃-his- in an α helix.[19] Histidine side chains separated by two or four amino acid residues in an undistorted α helix will, on the other hand, be incapable of participating in such a co-ordination mode. Force field calculations (MM2)[20] on the three peptides considered in this work indicate that the ligating histidine and methionine side chains should be suitably positioned for macrochelation in the most stable conformations (Fig. 1) of Hhis-gly-metH (β sheet) and Ac-his-ala-ala-ala-metH (α helix) but not in Ac-his-gly-gly-metH (β sheet). We selected L-alanine as the backbone residue for the pentapeptide Ac-his-ala-ala-ala-metH in view of its known propensity to stabilize an α helix.[17,18] Acetyl protection of the terminal amino group in the longer peptides simulates a backbone amide linkage and prevents the formation of $\kappa^2 N_{his}, N^3_{his}$ chelates in alkaline solution.

Results and discussion

Freshly mixed $[Pt(en)(H_2O)_2]^{2+}$–peptide reaction solutions for the determination of pH-dependent species distribution diagrams were brought to the required pH by addition of 0.1 M HNO_3 or NaOH. Following an incubation period of 28 d at 313 K in closed glass vessels under argon and subsequent registration of the final pH, such solutions were held at 277 K prior to analytical separation by reversed-phase HPLC in the presence of the ion-pairing agent pentafluoropropionic acid (PFP) and trifluoroacetic acid (TFA). The composition of the solutions was found to remain constant at this temperature over a period of several months. In the case of kinetic investigations, HPLC separations were performed under similar conditions after incubation at 313 K for specified periods of time. As demonstrated previously,[11,15,21] the kinetic inertness of platinum(II) complexes and the relatively short retention times involved for HPLC separations ($t_R < 100$ min) guarantee that elution of the reaction mixture at $298 < T < 313$ K and pH 2.1 will not lead to significant changes in species distribution. Where appropriate, ma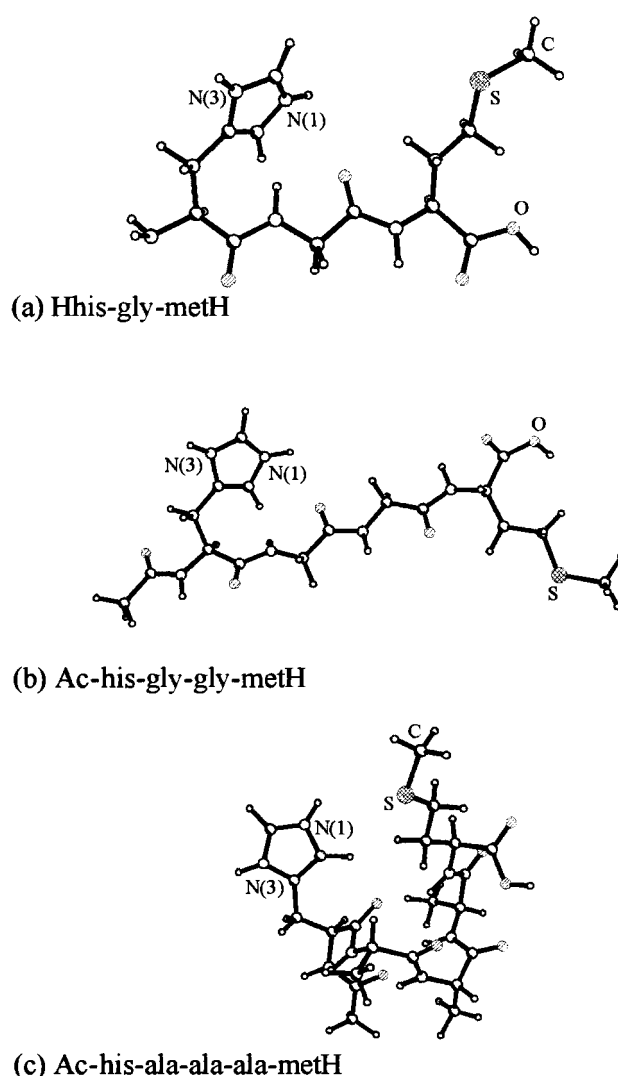jor products were separated by semi-preparative HPLC after incubation of reaction solutions for at least 14 d at 313 K. When analytical chromatograms indicated the predominance of one such complex, reaction solutions were prepared at the appropriate pH* (pH meter values uncorrected
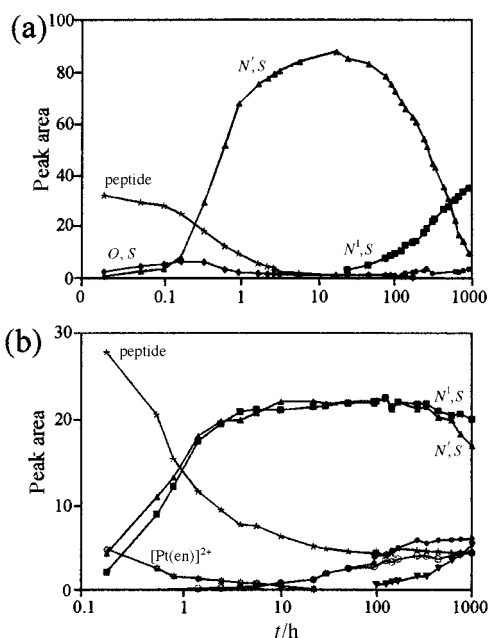
Fig. 2 Time dependence of product distribution in the 1:1 [Pt(en)-(H$_2$O)$_2$]$^{2+}$–Hhis-gly-metH reaction mixture as determined by HPLC (mobile phase 94–70% water–6–30% CH$_3$OH, ion-pairing agent 0.1% PFP, wavelength 220 nm) at (a) pH 2.99, (b) pH 8.52. Products: (a) ◆, 1:1 (O,S); ■ (N^1,S); ▲, 1:1 (N′,S); ●, 2:1 (N,N^3:N′,S); *, peptide; (b) ■, 1:1 (N^1,S); ▲, 1:1 (N′,S); ▼, 1:1 (N^3,N); ●, 2:1 (N,N^3:N′,S); ○, 2:1 (N,N^3:N^1,S); ☆, [Pt(en)]$^{2+}$; *, peptide.

Fig. 3 The ^{1}H NMR spectra of a equimolar [Pt(en)(D$_2$O)$_2$]$^{2+}$–Hhis-gly-metH reaction solution at pH* 3.0 and $T = 298$ K taken after (a) 20 and (b) 90 min.

for deuterium isotope effects in D$_2$O) for direct NMR measurements.

Major products were characterized by ^{1}H and ^{195}Pt NMR spectroscopy and FAB or ESI (electrospray) mass spectrometry. A downfield shift from *ca.* δ 2.1 for the free peptide to *ca.* δ 2.5 for a κS complex is characteristic for the δ-CH$_3$ protons adjacent to the methionine sulfur. An unambiguous assignment of the imidazole binding mode is generally possible on the basis of the ^{1}H–^{195}Pt coupling constants (measured at 80 MHz) for H^2 and H^5; ^3J values of *ca.* 17–20 Hz confirm N^1 co-ordination. A similar value is associated with H^2 in the case of N^3 binding but the ^4J(^{1}H–^{195}Pt) coupling constant for H^5 is now only *ca.* 8–10 Hz. Square-planar N$_4$ and N$_3$S co-ordination spheres can be distinguished for Pt^{II} on the basis of their typical ^{195}Pt chemical shifts in the respective ranges δ −2700 to −2900 and −3000 to −3300.[22]

L-Histidylglycyl-L-methionine

A time-dependent study of the 1:1 reaction between [Pt(en)-(H$_2$O)$_2$]$^{2+}$ and the dipeptide Hhis-metH at 313 K and pH 4.55 demonstrated that an intermediate κ^{2}O,S chelate is formed very rapidly, only to convert into two major species, namely κ^{2}N^1,S and κ^{2}N′$_{met}$,S complexes, within 5 h.[15] After reaching a quasi-stationary state (*ca.* 50 h) the latter complex slowly isomerizes into the presumably more stable κ^{2}N$_{his}$,N′$_{met}$ five-membered chelate, which then predominates after 600 h.

To elucidate the reaction pathways for [Pt(en)]$^{2+}$ interaction with the analogous tripeptide Hhis-gly-metH, we have studied the time dependence of product distribution both at low pH (2.99) and in weakly alkaline solution (pH 8.52). As depicted in Fig. 2(a), it is once again possible to detect a κ^{2}O,S intermediate after short incubation times ($t \le 3$ h) in acid solution. Although the low concentration and rapid conversion of this initial species into the thermodynamically preferred κ^{2}N′$_{met}$,S six-membered chelate prevent its satisfactory semipreparative separation, strong evidence for the designated co-ordination mode is provided by the 400 MHz ^{1}H NMR spectra, taken for an equimolar [Pt(en)(D$_2$O)$_2$]$^{2+}$–Hhis-gly-metH reaction solution after respectively 20 and 90 min at pH* 3.0 and $T = 298$ K (Fig.
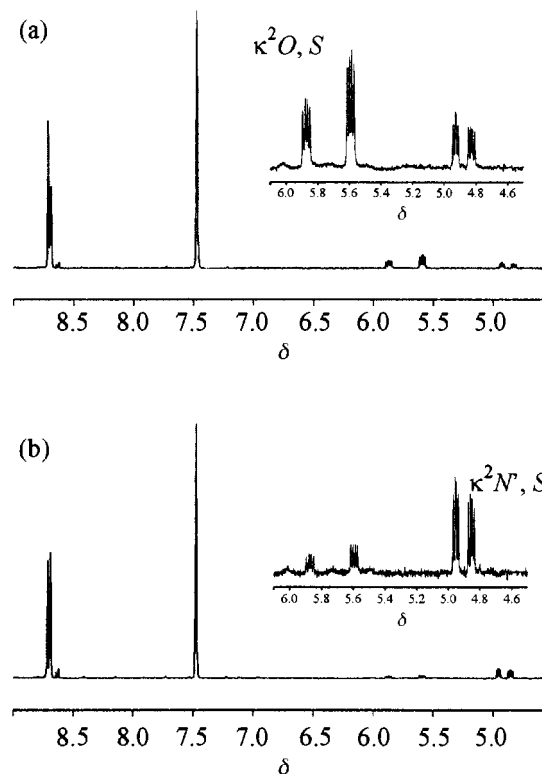
3). Pronounced downfield shifts to δ 5.33 and 5.58 have been reported by Appleton *et al.*[22] for the α-proton in *cis*-[Pt(NH$_3$)$_2$-(Hmet-κ^{2}O,S)]$^{2+}$, values that are similar to those of respectively δ 5.59/5.87 and δ 5.60/5.89 for the diastereomers of [Pt(en)-(H$_3$his-gly-met-κ^{2}O,S)]$^{3+}$ (Scheme 1) and [Pt(en)(H$_2$his-met-κ^{2}O,S)]$^{2+}$.[15] As may be seen in Fig. 3(b), the integral values of these resonances rapidly decrease in comparison to those at δ 4.86/4.94, which belong to the κ^{2}N′$_{met}$,S complex. Thioether co-ordination in the intermediate κ^{2}O,S species is confirmed by the downfield shift of its methionine δ-CH$_3$ protons to δ 2.51.

A crucial anchoring role is apparent for the methionine S in directing the reaction pathway to the thermodynamically preferred 15-membered κ^{2}N^1$_{his}$,S macrochelate at low pH. Following initial formation of the κ^{2}O,S intermediate, a relatively fast metallation reaction leads to replacement of the kinetically favoured carboxyl O by its neighbouring methionine amide N in [Pt(en)(H$_3$his-gly-met-κ^{2}N$_{met}$,S)]$^{3+}$, a six-membered chelate that clearly predominates at pH 2.99 after 10 h. In the final stage of the reaction pathway illustrated in Scheme 1 this complex slowly isomerizes in a first-order reaction [rate constant $k = 0.8(2) \times 10^{-6}$ s^{-1}] to the κ^{2}N^1$_{his}$,S macrochelate, which provides the major product after 500 h. An alternative terminal κ^{2}N$_{his}$,N^3$_{his}$ chelation of a second [Pt(en)]$^{2+}$ fragment affords the 2:1 1κ^{2}N$_{his}$,N^3$_{his}$:2κ^{2}N′$_{met}$,S complex as a minor species over a similar long incubation period at 313 K.

Typical pK_a values for the first deprotonation of an imidazole N in histidine-containing peptides lie in the range 6.7–7.1.[23] This indicates that raising the pH of an equimolar [Pt(en)-(H$_2$O)$_2$]$^{2+}$–Hhis-gly-metH reaction system to provide a weakly alkaline solution should greatly accelerate the rate of N^1 (or N^3) co-ordination. Comparison of the time dependent species distributions at pH values of 2.99 and 8.52 (Fig. 2) confirm that this is indeed the case. At the higher pH, κ^{2}N^1$_{his}$,S macrochelation is kinetically competitive with formation of the six-membered κ^{2}N′$_{met}$,S chelate and both complexes reach their maximum concentrations after *ca.* 10 h. As previously discussed for the acid solution depicted in Fig. 2(a), the histidine residue of the latter compound is capable of co-ordinating a

$\kappa^2 O,S$

$t_{max} = 0.25$ h

$\kappa^2 N'_{met},S$

$t_{max} = 20$ h
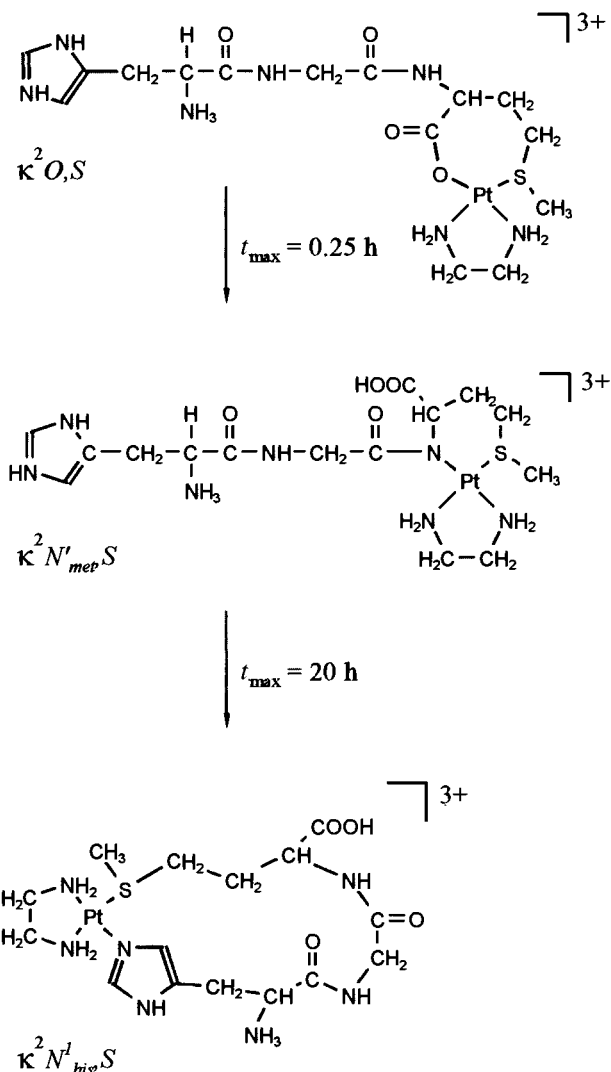
$\kappa^2 N^1_{his},S$

Scheme 1 Reaction pathway for the formation of the 15-membered $\kappa^2 N^1_{his},S$ macrochelate at pH 2.99.

Fig. 4 Chromatograms for the 1:1 [Pt(en)(H$_2$O)$_2$]$^{2+}$–Hhis-gly-metH reaction system at pH 8.52 (ion-pairing agent 0.1% PFP, pH 2.1, detection wavelength = 220 nm) for (a) $t = 0.8$ h, mobile phase 87% water–13% CH$_3$OH, (b) $t = 1.45$ h, mobile phase 87% water–13% CH$_3$OH, (c) $t = 960$ h, mobile phase 93% water–7% CH$_3$OH.

Fig. 5 Time dependence of product distribution in the 2:1 [Pt(en)-(H$_2$O)$_2$]$^{2+}$–Hhis-gly-metH reaction mixture as determined by HPLC (mobile phase 94–70% water–6–30% CH$_3$OH, ion-pairing agent 0.1% PFP, wavelength 220 nm) at pH 9.37. Products: ■, 1:1 (N^1,S); ▲, 1:1 (N',S); ○, 2:1 ($N,N^3:N',S$); ●, 2:1 ($N,N^3:N^1,S$); ☆, [Pt(en)]$^{2+}$; *, peptide.

second metal fragment to provide the dinuclear $1\kappa^2 N_{his}$, $N^3_{his}:2\kappa^2 N'_{met},S$ complex, which reaches an effectively quasi-stationary state after *ca.* 100 h. This state of affairs is accompanied by a slow decrease in the concentration of its $\kappa^2 N'_{met},S$ precursor complex and a concomitant increase in the concentration of the $\kappa^2 N_{his},N^3_{his}$ decay product over the time period 100–1000 h, thereby allowing the formulation of the following reaction pathway: $\kappa^2 N'_{met},S \longrightarrow 1\kappa^2 N_{his},N^3_{his}:2\kappa^2 N'_{met},S \longrightarrow \kappa^2 N_{his},N^3_{his}$. Chromatograms [*e.g.* Fig. 4(c), $t = 960$ h] taken after an incubation period of $t > 100$ h also contain the retention peak of a second minor dinuclear complex, whose $1\kappa^2 N_{his},N^3_{his}:2\kappa^2 N^1_{his},S$ co-ordination mode requires the 15-membered $\kappa^2 N^1_{his},S$ macrochelate as its precursor.

These proposed reaction pathways are confirmed by a time dependent study of product formation in a 2:1 reaction solution of [Pt(en)(H$_2$O)$_2$]$^{2+}$ and Hhis-gly-metH at pH 9.37, the results of which are summarized in Fig. 5. Co-ordination of a second Pt^{II} is much more rapid in the presence of an initial excess of the transition metal fragment and significant concentrations of the dinuclear complexes can be detected in analytical chromatograms after only a few hours. Interestingly the $1\kappa^2 N_{his},N^3_{his}:2\kappa^2 N'_{met},S$ complex now provides the thermodynamically preferred species at this relatively high pH value. In contrast, the concentration of the second $1\kappa^2 N^1_{his},N^3_{his}:2\kappa^2-N'_{met},S$ dinuclear complex reaches a maximum after an incubation time of *ca.* 100 h at 313 K and then slowly falls in the subsequent time period 100–672 h. This state of affairs is also reflected in the pH dependent product distribution diagram for
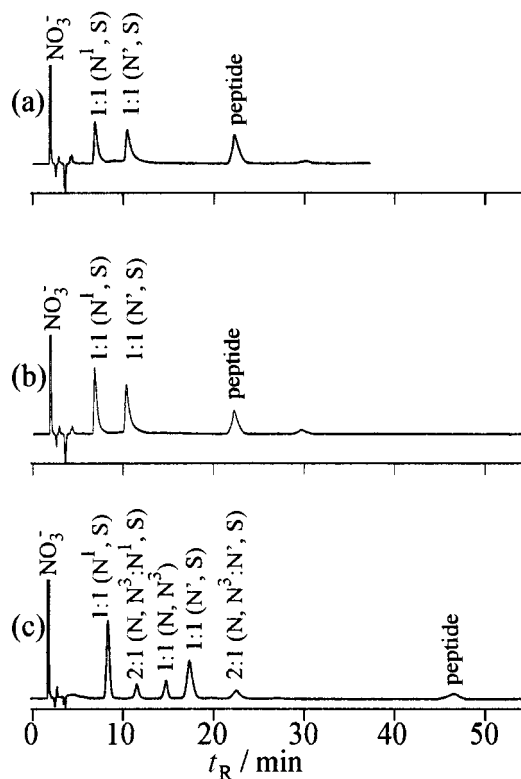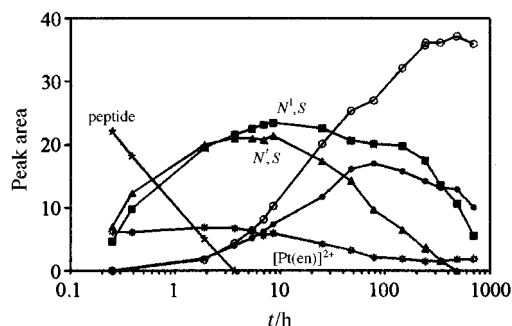
the 1:1 [Pt(en)(H$_2$O)$_2$]$^{2+}$–Hhis-gly-metH reaction system after 28 d at 313 K, that is presented in Fig. 6.

Both of the major dinuclear complexes and the $\kappa^2 N^1_{his},S$ macrochelate could be successfully separated by semipreparative HPLC and fully characterized by ^{1}H and ^{195}Pt NMR in addition to FAB or ESI mass spectrometry. Their purity was monitored by analytical HPLC traces. As the six-membered $\kappa^2 N'_{met},S$ chelate is the only product present in a 1:1 reaction solution after 10 h at 313 K and pH 2.99, it was prepared under these conditions for subsequent NMR and MS characterization. Spectroscopic data for the four Hhis-gly-metH complexes are listed in Table 1.

Confirmation of an N$_3$S environment for Pt^{II} in both mononuclear complexes is provided by their respective ^{195}Pt NMR chemical shifts of δ −3225 and −3212. The downfield shifts of the methionine δ-CH$_3$ methyl ^{1}H NMR resonances from δ 2.08 for the free tripeptide to 2.51 for the $\kappa^2 N'_{met},S$ complex and 2.39

Table 1 The ^1H and ^{195}Pt NMR chemical shifts δ, J values (in Hz) and mass spectral base peaks for complexes separated for the 1:1 and 2:1 [Pt(en)(H$_2$O)$_2$]$^{2+}$–Hhis-gly-metH reaction systems

	$\kappa^2 N'_{met},S$	$\kappa^2 N^1_{his},S$	$1\kappa^2 N_{his}N^3_{his}:2\kappa^2 N'_{met},S$	$1\kappa^2 N_{his},N^3_{his}:2\kappa^2 N^1_{his},S$
H^2	8.69 (s)	8.14 (s), $^3J = 19$	7.91 (s), $^3J = 18$	7.41 (s), $^3J = 14$
H^5	7.47 (s)	6.95 (s), $^3J = 9$	7.11 (s), $^4J = 9$	6.73 (s), $^3J = 19$, $^4J = 9$
CH-α_{his}	4.45 (m)	4.38 (m)	3.69 (m)	3.79 (m)
CH$_2$-β_{his}	3.45 (m)	3.39, 3.42 (2dd)	3.04, 3.15 (2dd)	3.10 (m)
CH-α_{met}	4.97 (m)	4.75 (m)	4.78 (m)	4.62 (m)
CH$_2$-β_{met}	2.2, 2.7 (m)	2.13 (br)	2.43 (br)	1.92, 2.30 (m)
CH$_2$-γ_{met}	2.6 (m)	2.57 (m)	2.7 (m)	2.4 (m)
CH$_3$-δ_{met}	2.51 (s)	2.39 (s)	2.52 (s)	2.5 (s)
CH$_2$-α_{gly}	4.07 (dd)	4.21, 4.63 (2d)	4.31, 4.51 (2d)	4.11, 4.51 (2d)
CH$_2$ of en	2.8 (br)	2.8 (br)	2.78 (br)	2.8 (br)
$\delta(^{195}Pt)$	-3225	-3212	$-2880, -3301$	$-2865, -3209$
pH*	3.0	1.6	1.6	1.6
MS base peak (*m/z*)	598 (ESI)	600 (FAB)^a	851, 426 (ESI)	851, 426 (ESI)

^{a} H/D Exchange.

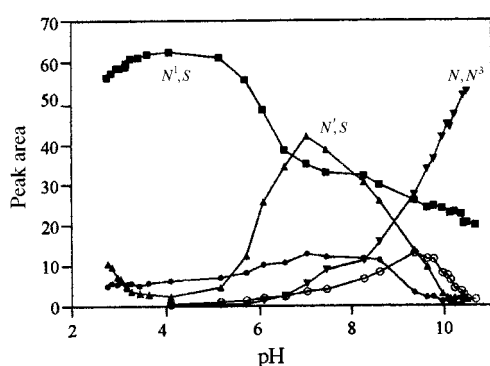**Fig. 6** Product distribution for the 1:1 [Pt(en)(H$_2$O)$_2$]$^{2+}$–Hhis-gly-metH reaction system after 28 d at 313 K as determined by HPLC (mobile phase 96–89% water–4–11% CH$_3$OH, ion-pairing agent 0.1% PFP, pH 2.1, $T = 298$ K, wavelength 220 nm) for the range $2.8 < \text{pH} < 10.8$. Products: ■, 1:1 (N^1,S); ▲, 1:1 (N',S); ▼, 1:1 (N,N^3); ●, 2:1 ($N,N^3:N',S$); ⊖, 2:1 ($N,N^3:N^1,S$).

for the $\kappa^2 N^1_{his},S$ macrochelate are also typical for thioether sulfur co-ordination. Whereas the histidine protons H^2 and H^5 of the former 6-membered chelate exhibit ^1H NMR δ values of 8.69 and 7.47, that are characteristic for a doubly protonated imidazole ring in acid solution, the high-field shifts of the analogous H atoms in the 15-membered $\kappa^2 N^1_{his},S$ macrochelate confirm the participation of the heteroaromatic ring in platinum(II) co-ordination. N^1 Binding is indicated by the similarity of the ^1H–^{195}Pt coupling constants (19 Hz) for both ring protons.

The nuclearity of the 2:1 complexes was established both by ESI MS and by ^{195}Pt NMR spectroscopy. In addition to M$^+$ and M^{2+} peaks at m/z 851 and 426, intense [M + PFP]$^+$ (m/z 1016) and [M + 2PFP]$^+$ (m/z 1179) ions can also be identified in the mass spectrum of the $1\kappa^2 N_{his},N^3_{his}:2\kappa^2 N^1_{his}:S$ complex [Fig. 7(b)]. The presence of both N$_4$ and N$_3$S platinum(II) co-ordination spheres is indicated for the dinuclear complexes by their ^{195}Pt singlets at respectively $\delta -2880/-3301$ and $-2865/-3209$. Typical high-field imidazole H^2 and H^5 ^1H NMR shifts and lowfield δ-CH$_3$ shifts confirm the involvement of both potentially ligating side chains in metal binding. Whereas the ^4J value of 9 Hz for H^5 is in accordance with exclusively imidazole N^3 co-ordination in the $1\kappa^2 N_{his},N^3_{his}:2\kappa^2 N'_{met},S$ complex, whose structure is depicted in Fig. 7(a), the ^3J and ^4J values of respectively 19 and 9 Hz for the analogous proton suggest that both imidazole nitrogen atoms must participate in platinum(II) co-ordination in the second $1\kappa^2 N_{his},N^3_{his}:2\kappa^2 N^1_{his},S$ dinuclear species [Fig. 7(b)].

Ac-his-gly-gly-metH

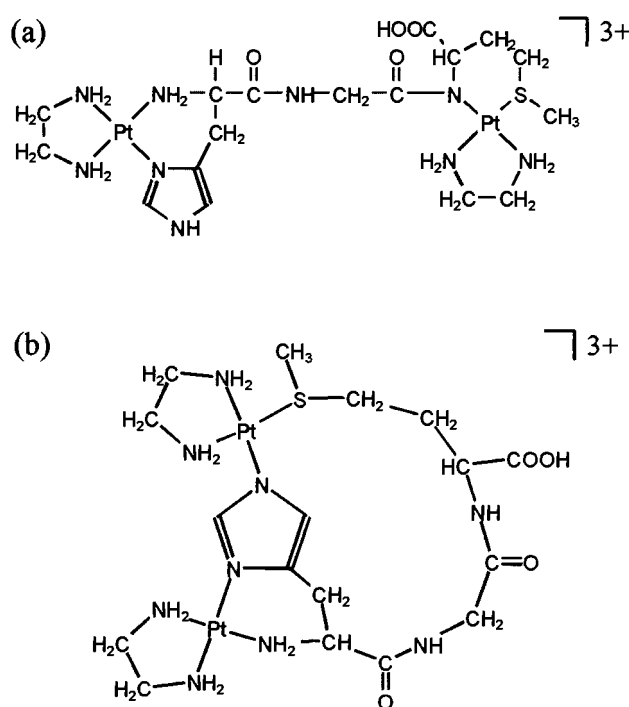The complete absence of a $\kappa^2 N^3_{his},S$ macrochelate in the

Fig. 7 Structures of the dinuclear complexes (a) [{Pt(en)}$_2$(μ-Hhis-gly-met-1$\kappa^2 N_{his},N^3_{his}:2\kappa^2 N'_{met},S$)]$^{3+}$ and (b) [{Pt(en)}$_2$(μ-his-gly-met-1$\kappa^2 N_{his},N^3_{his}:2\kappa^2 N^1_{his},S$)]$^{3+}$.

[Pt(en)(H$_2$O)$_2$]$^{2+}$–Hhis-gly-metH reaction system is remarkable, in view of the preference for N^3 established by Appleton *et al.*[16] for competing linkage isomers of the type [Pt(dien)(Hhis)]$^{2+}$. However, we ourselves have demonstrated[14] that [Pt(dien)]$^{2+}$ clearly prefers the imidazole N^1 binding site, following its migration from the thioether sulfur atom of the dipeptide Hhis-metH at pH >6. Inspection of Fig. 1(a) also indicates that N^1 will be orientated towards the methionine side-chain in the energetically most favourable conformation of Hhis-gly-metH. In contrast, the potentially ligating side-chains are positioned on opposite sides of the peptide backbone of Ac-his-gly-gly-metH [Fig. 1(b)], suggesting not only that the speed of $\kappa^2 N^1_{his},S$ or $\kappa^2 N^3_{his},S$ macrochelation should be significantly slower than for the former tripeptide, but also that the second imidazole binding site N^3 might be more competitive than in the shorter peptide.

The results of our pH and time dependent HPLC investigation of the equimolar [Pt(en)(H$_2$O)$_2$]$^{2+}$–Ac-his-gly-gly-metH reaction system are illustrated in Fig. 8. Following initial $\kappa^2 O,S$ chelation, as also observed for the shorter peptides Hhis-metH[15] and Hhis-gly-metH [Fig. 2(a)], rapid substitution of the carboxyl O by the neighbouring methionine amide N leads
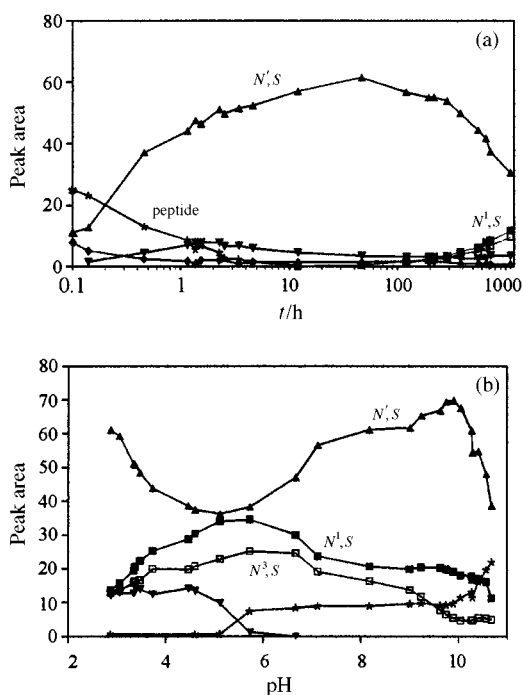
Fig. 8 (a) Time dependence of product distribution in the 1:1 [Pt(en)-(H₂O)₂]²⁺–Ac-his-gly-gly-metH reaction mixture as determined by HPLC (mobile phase 93–75% water–7–25% CH₃OH, ion pairing agent 0.1% PFP, pH 2.1, $T = 298$ K, wavelength 220 nm) at pH 2.70. (b) Product distribution of the above system after 28 d at 313 K as determined by HPLC (conditions as above) for the range $2.7 < \text{pH} < 10.8$ (mp = minor product). Products: ■, 1:1 (N^1,S); ◆, 1:1 (O,S); ▲, 1:1 (N',S); □, 1:1 (N^3,S); ▼, mp; *, peptide.

to formation of [Pt(en)(Ac-his-gly-gly-met-κ^2N_{met},S)]²⁺ at pH 2.70. As a result of the unfavourable siting of the ligating histidine and methionine residues on opposite sides of the tetrapeptide backbone, isomerization of this six-membered chelate to imidazole co-ordinated macrochelates proceeds at a significantly slower rate than for Hhis-gly-metH. Fig. 8(a) indicates that the $\kappa^2N'_{\text{met}}$,S complex reaches a concentration maximum after *ca.* 50 h but still predominates in the incubation solution at 313 K after 1000 h. In contrast to the analogous tripeptide, Hhis-gly-metH, formation of the respectively 17- and 18-membered $\kappa^2N^3_{\text{his}}$,S and $\kappa^2N^1_{\text{his}}$,S macrochelates (Fig. 9) is competitive at pH 2.70 and this is indeed the case over the wide range $2.7 < \text{pH} < 10.8$. As illustrated in the pH dependent product distribution diagram, Fig. 8(b), $\kappa^2N'_{\text{met}}$,S co-ordination is also clearly favoured in alkaline solution, in which formation of macrochelates is much more rapid, leading to a quasi-stationary state of affairs after *ca.* 10 h. Significant concentrations of dinuclear complexes could not be detected in analytical chromatograms.

All three mononuclear products were separated by semi-preparative HPLC and fully characterised. As for the [Pt(en)-(H₂O)₂]²⁺–Hhis-gly-metH reaction system, the $\kappa^2N^1_{\text{his}}$,S macrochelate exhibits a shorter retention time than the $\kappa^2N'_{\text{met}}$,S chelate, which is now followed by the second macrochelate. The ¹H and ¹⁹⁵Pt NMR data for the Hhis-gly-gly-metH complexes are presented in Table 2. The presence of N₃S co-ordination spheres in these platinum(ɪɪ) compounds is confirmed by their very similar ¹⁹⁵Pt NMR chemical shifts of δ −3201 ($\kappa^2N'_{\text{met}}$,S), −3213 ($\kappa^2N^1_{\text{his}}$,S) and −3184 ($\kappa^2N^3_{\text{his}}$,S). An assignment of the nitrogen binding mode is once again straightforward on the basis of the ¹H NMR δ values and ¹H–¹⁹⁵Pt coupling constants for the imidazole ring protons H² and H⁵. Co-ordination at N¹ in [Pt(en)(Ac-his-gly-gly-metH-$\kappa^2N^1_{\text{his}}$,S)]²⁺ is indicated by the presence of similar ³J values of 19 Hz for both protons in an 80 MHz spectrum, N³ in [Pt(en)(Ac-his-gly-gly-metH-$\kappa^2N^3_{\text{his}}$,S)]²⁺ by the observation of strikingly different coupling constants of 18 and 9 Hz for H²

Table 2 The ¹H and ¹⁹⁵Pt NMR chemical shifts δ, J values (in Hz) and mass spectral base peaks for complexes separated for the 1:1 [Pt(en)(H₂O)₂]²⁺–Ac-his-gly-gly-metH reaction system

	$\kappa N'_{\text{met}}$,S	$\kappa^2N^1_{\text{his}}$,S	$\kappa^2N^3_{\text{his}}$,S
H²	8.62 (s)	8.07 (s), ³J = 19	8.06 (s), ³J = 18
H⁵	7.31 (s)	7.21 (s), ³J = 19	7.19 (s), ⁴J = 9
CH₃-Ac	2.00 (s)	2.03 (s)	1.98 (s)
CH-α$_{\text{his}}$	4.8 (m)	4.75 (m)	4.8 (m)
CH₂-β$_{\text{his}}$	3.15, 3.30 (2dd)	3.22 (m)	2.82, 3.47 (m)
CH-α$_{\text{met}}$	4.8 (m)	4.8 (m)	4.5 (m)
CH₂-β$_{\text{met}}$	2.27, 2.44 (m)	2.2, 2.3 (m)	2.29, 2.45 (m)
CH₂-γ$_{\text{met}}$	2.75 (m)	2.8 (m)	3.05 (m)
CH₃-δ$_{\text{met}}$	2.44 (s)	2.28 (s)	2.61 (s)
CH₂-α$_{\text{gly}}$	3.99 (m)	3.89 (m)	3.84, 4.02 (2dd)
CH₂ of en	2.7 (br)	2.8 (br)	2.8 (br)
δ(¹⁹⁵Pt)	−3201	−3213	−3184
pH*	3.0	1.6	1.6
MS base peak (m/z)	698 (FAB)	698 (FAB)	698 (FAB)
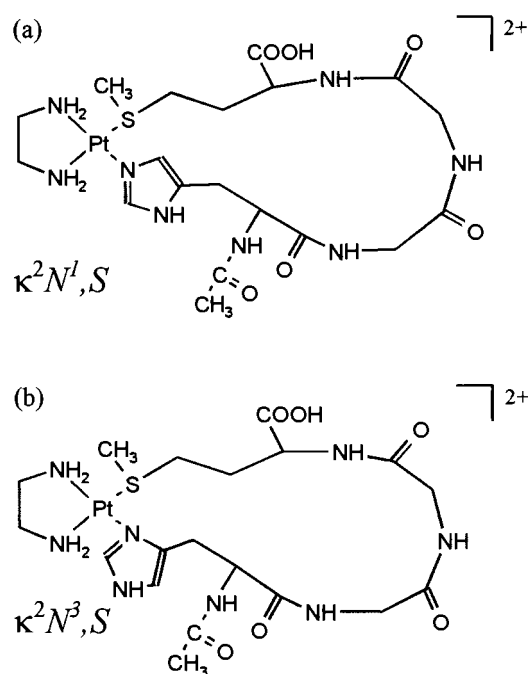
Fig. 9 Structures of the $\kappa^2N^1_{\text{his}}$,S and $\kappa^2N^3_{\text{his}}$,S macrochelates formed between [Pt(en)]²⁺ and Ac-his-gly-gly-metH.

and H⁵. The chemical shifts of the imidazole protons in the six-membered $\kappa^2N'_{\text{met}}$,S chelate are similar to those of the analogous Hhis-gly-metH complex and typical for a doubly protonated heteroaromatic ring.

Ac-his-ala-ala-ala-metH

Peptides with potentially ligating side chains at their *i* and *i* + 4 positions should be capable of chelating metal ions when their backbones adopt an α helix, as depicted in Fig. 1(c) for Ac-his-ala-ala-ala-metH. This suggests that the rate of formation of imidazole co-ordinated macrochelates should be more rapid for this pentapeptide than for the tetrapeptide Ac-his-gly-gly-metH, a hypothesis that is confirmed by the product distribution diagram presented in Fig. 10. Comparison of this Figure with Fig. 8(b) (Ac-his-gly-gly-metH) indicates that the concentration ratios of the three competing mononuclear platinum(ɪɪ) complexes are effectively the same in alkaline solution for the tetra- and penta-peptide. As demonstrated in Fig. 2(b) for Hhis-gly-metH, formation of the $\kappa^2N'_{\text{met}}$,S chelate and the competing $\kappa^2N^1_{\text{his}}$,S macrochelate proceeds at a similar rate under such conditions, leading to a quasi-stationary state after only *ca.* 10 h. In contrast to the tripeptide, the former complex is clearly

Table 3 HPLC Conditions for semipreparative separation of platinum(II) complexes after incubation of $[Pt(en)(H_2O)_2]^{2+}$ with histidine- and methionine-containing peptides at 313 K for 28 d

| Molar ratio Pt^II : peptide	pH (after 28 d)	% CH₃OH in mobile phase	% (v/v) IPR	$t_R{}^a$/min	Co-ordination mode
Hhis-gly-metH 1 : 1	7.6	4	0.1 PFP	10	$\kappa^2 N^1_{met},S$
				29	$\kappa^2 N'_{met},S$
				34	$\kappa^2 N_{his},N^3_{his}$
Hhis-gly-metH 2 : 1	6.3	4	0.1 PFP	15	$1\kappa^2 N_{his},N^3_{his}:2\kappa^2 N^1_{his},S$
				40	$1\kappa^2 N_{his}N^3_{his}:2\kappa^2 N'_{met},S$
Ac-his-(gly)₂-metH 1 : 1	5.2	7	0.1 PFP	10	$\kappa^2 N^1_{his},S$
				18	$\kappa^2 N'_{met},S$
				21	$\kappa^2 N^3_{his},S$
Ac-his-(ala)₃-metH 1 : 1	5.5	5	0.073 TFA	13	$\kappa^2 N'_{met},S$
				15	$\kappa^2 N^1_{his},S$
				17	$\kappa^2 N^3_{his},S$

^{a} Analytical separations.
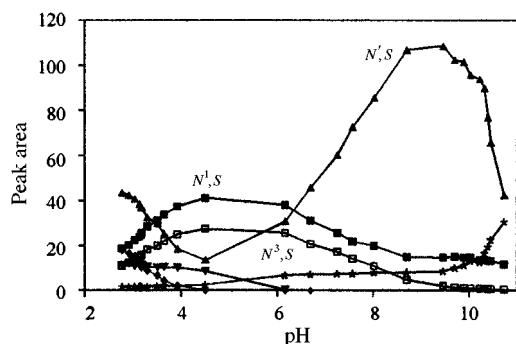
Fig. 10 Species distribution for the equimolar $[Pt(en)(H_2O)_2]^{2+}$–Ac-his-(ala)₃-metH reaction system after 28 d at 313 K as determined by HPLC (mobile phase 95–80% water–5–20% CH₃OH, ion-pairing agent 0.073% TFA, pH 2.1, $T = 298$ K, wavelength 220 nm), mp = minor product. Products: ◆, 1 : 1 (O,S); ▲, 1 : 1 (N′,S); ■, 1 : 1 (N¹,S); □, 1 : 1 (N³,S); *, peptide; ▼, mp.

Table 4 The ^{1}H and ^{195}Pt NMR chemical shifts δ, J values (in Hz) and mass spectral base peaks for complexes separated for the 1 : 1 $[Pt(en)(H_2O)_2]^{2+}$–Ac-his-(ala)₃-metH reaction system

	$\kappa^2 N'_{met},S$	$\kappa^2 N^1_{his},S$	$\kappa^2 N^3_{his},S$
H²	8.63 (s)	8.05 (s), $^3J = 18$	8.13 (s), $^3J = 16$
H⁵	7.31 (s)	7.08 (s), $^3J = 19$	7.21 (s), $^4J = 9$
CH₃-Ac	2.00 (s)	2.07 (s)	2.03 (s)
CH-α_his	4.66 (m)	4.8 (m)	4.8 (m)
CH₂-β_his	3.15, 3.24 (2dd)	3.13 (m)	3.5 (m)
CH-α_met	4.6 (m)	4.5 (m)	4.8 (m)
CH₂-β_met	2.3, 2.5 (m)	2.16, 2.36 (m)	2.15 (m)
CH₂-γ_met	2.7 (m)	2.72 (m)	3.85 (m)
CH₃-δ_met	2.40 (s)	2.36 (s)	2.36 (s)
CH-α_ala	4.31 (m)	3.93, 4.22, 4.31 (m)	4.3 (br)
CH₃-β_ala	1.39	1.40	1.41
CH₂ of en	2.7 (br)	2.81 (br)	2.84 (br)
$\delta(^{195}$Pt)	−3201	−3213	−3226
pH*	1.6	1.5	1.8
MS base peak (m/z)	910^a (FAB)	795 (FAB)	795 (FAB)

^{a} $[Pt(en)\{Ac\text{-}his\text{-}(ala)_3\text{-}met\text{-}\kappa^2 N'_{met},S\}(TFA)]^+$.

thermodynamically favoured at pH > 7 for both the tetra- and penta-peptide. Metallation of the methionine amide nitrogen is also relatively rapid at low pH values, following initial thioether S anchoring in a $\kappa^2 O,S$ six-membered chelate. The product ratio in the range 2.7 < pH < 6 after an incubation period of 28 d at 313 K now depends on the rate of isomerization of the $\kappa^2 N'_{met},S$ chelate to the larger $\kappa^2 N^1_{his},S$ and $\kappa^2 N^3_{his},S$ macro-chelates (Fig. 11). This process is accelerated in Ac-his-ala-ala-ala-metH in comparision to Ac-his-gly-gly-metH, as a result of the proximity of the ligating side chains in the energetically favourable α helix, with the result that the macrochelates now predominate in the range 3.7 < pH < 5.7 in Fig. 10. As for the tetrapeptide, significant concentrations of dinuclear complexes could not be detected by analytical HPLC.

Separation of the three mononuclear products was once again possible using semipreparative HPLC, in this case with TFA as the ion-pairing agent. This led to a change in the elution sequence (Table 3) with the $\kappa^2 N^1_{his},S$ macrochelate now exhibiting a longer retention time than the competing $\kappa^2 N'_{met},S$ chelate. Spectroscopic data for the three Ac-his-ala-ala-ala-metH complexes are summarized in Table 4. Typical ^{1}H NMR downfield shifts for the thioether δ-CH₃ protons (δ 2.36–2.40) and ^{195}Pt NMR δ values in the range −3201 to −3226 confirm their methionine sulfur co-ordination. Assignment of the imidazole binding mode in the respectively 20- and 21-membered $\kappa^2 N^3_{his},S$ and $\kappa^2 N^1_{his},S$ macrochelates is once again based on the values of the ^{1}H–^{195}Pt coupling constants for the imidazole ring protons H² and H⁵.

Conclusion

Our present time and pH dependent HPLC analyses of the reaction between $[Pt(en)(H_2O)_2]^{2+}$ and histidine- and

$\kappa^2 N^1,S$

$\kappa^2 N^3,S$

Fig. 11 Structures of (a) $[Pt(en)\{Ac\text{-}his\text{-}(ala)_3\text{-}metH\text{-}\kappa^2 N^1_{his},S\}]^{2+}$ and (b) $[Pt(en)\{Ac\text{-}his\text{-}(ala)_3\text{-}metH\text{-}\kappa^2 N^3_{his},S\}]^{2+}$.

methionine-containing tri-, tetra- and penta-peptides once again confirm the well documented kinetic preference of Pt^II for methionine S. Formation of both the $\kappa^2 N'_{met},S$ six-membered

chelate and the competing imidazole co-ordinated $\kappa^2 N^1_{his}, S$ or $\kappa^2 N^3_{his}, S$ macrochelates (the latter species only for the longer peptides) proceed at a similar relatively rapid rate in alkaline solution, leading to a quasi-stationary species distribution after *ca.* 10 h at 313 K. Although the positions of the ligating residues in the peptide chain, therefore, appear to exhibit little influence on the rate of formation of the possible products at pH > 7, a clear thermodynamic preference for the smaller $\kappa^2 N'_{met}, S$ chelate of the C-terminal methionine residue is apparent for the longer tetra- and penta-peptides. Likewise, whereas, the $\kappa^2 N^1_{his}, S$ and $\kappa^2 N^3_{his}, S$ macrochelates exhibit similar relative concentrations over the complete range 2.7 < pH < 10.8 for $i + 3$ and $i + 4$ spacings of the ligating side chains, no HPLC evidence could be obtained for the presence of a $\kappa^2 N^3_{his}, S$ macrochelate in the [Pt(en)(H$_2$O)$_2$]$^{2+}$–Hhis-gly-metH reaction systems. As we have previously reported, exclusive formation of a $\kappa^2 N^1_{his}, S$ macrochelate for the [Pt(en)(H$_2$O)$_2$]$^{2+}$–Hhis-metH reaction system is also observed under similar conditions.[15] Our present findings, therefore, suggest that a N^1_{his}/N^3_{his} dichotomy is only relevant for macrochelates formed by peptides with two or more residues between competing ligating histidine and methionine side chains.

In contrast to alkaline solutions, a clear kinetic preference for $\kappa^2 N'_{met}, S$ chelation of the C-terminal methionine residue could be established for all peptides considered in this work at pH < 4. Following initial anchoring on the thioether S in a $\kappa^2 O, S$ complex, metallation of the neighbouring amide nitrogen is once again relatively rapid under these conditions. The final product distribution after 28 d incubation at 313 K now depends, in the pH range 2.7–5.5 [Fig. 6, 8(b) and 10], on the rate of slow isomerization of this six-membered $\kappa^2 N'_{met}, S$ chelate to the thermodynamically more stable imidazole co-ordination macrochelates. The rate of this reaction is clearly influenced by the positions of the ligating histidine and methione residues in the peptide chain. Formation of macrochelates is more rapid at an $i + 4$ spacing, which brings the participating thioether S and imidazole N donor atoms into close proximity after one turn of an α helix, than at an $i + 3$ spacing, for which the energetically favoured β sheet places the ligating side chains on opposite sides of the peptide backbone.

In view of the fact that Pt^{II} is known to exhibit an *in vivo* half-life of several days after administration of cisplatin,[24] our findings suggest that the close proximity of histidine residues to kinetically favoured methionine side-chains could prevent the release of the drug from an intracellular protein-bound reservoir.

Experimental

Materials

The complex [PtCl$_2$(en)] was prepared in accordance with literature procedures.[25] The peptides Hhis-gly-metH, Ac-his-gly-gly-metH and Ac-his-ala-ala-ala-metH were synthesized by Dr Kalbacher of the Medizinisch-Naturwissenschaftliches Forschungszentrum at the University of Tübingen and used as received. HPLC-Grade methanol was from J. T. Baker and Merck, pentafluoropropionic acid and trifluoroacetic acid from Fluka or Aldrich. Stock solutions (4 mmol dm^{-3}) of [Pt(en)-(H$_2$O)$_2$]$^{2+}$ for analytical HPLC were prepared by stirring an aqueous mixture of [PtCl$_2$(en)] with the required equivalent of AgNO$_3$ (1 : 1.96) for 24 h in the dark followed by centrifugation of the AgCl precipitate at 277 K. The 15 or 80 mmol dm^{-3} solutions of respectively [Pt(en)(H$_2$O)$_2$]$^{2+}$ (semipreparative HPLC) and [Pt(en)(D$_2$O)$_2$]$^{2+}$ (NMR) were obtained by an analogous procedure.

HPLC

The analytical separations were performed with the following chromatographic equipment: either a Merck L-7100 ternary gradient pump, Rheodyne 7125 sample injector, Merck column thermostat L-7360 and UV detector L-7400, or a Knauer MAXI-STAR ternary gradient pump, Rheodyne 7125 sample injector and Merck variable-wavelength UV/VIS detector L-4250. Semipreparative work was carried out with a Knauer 64 pump, A0258 sample injector and Merck L-4000A UV detector. Integration and evaluation were performed with the Knauer Eurochrom 2000 software package. Reversed-phase columns (25 × 0.4 cm inside diameter) for analytical separations were packed with Nucleosil 100-C$_{18}$ (5 μm, Macherey-Nagel); 25 × 2 cm inside diameter reversed-phase columns (Nucleosil 100-C$_{18}$, 10 μm) were employed for semipreparative work. Analytical (0.8 mmol dm^{-3} per equivalent) and semipreparative (6 mmol dm^{-3} per equivalent) reaction solutions were prepared at required Pt^{II} : peptide molar ratios (1 : 1, 2 : 1). The initial pH was adjusted by addition of 0.1 mol dm^{-3} HNO$_3$ or NaOH and the resulting solutions were incubated at 313 K for the required period of time. After registration of the final pH, such solutions were held at 277 K prior to HPLC separation. Samples were run isocratically or with a one-step gradient using 75–100% water–0–25% methanol as the mobile phase (pH 2.1 ± 0.1) at column temperatures between 293 and 313 K in the presence of 0.1% (v/v) PFP or 0.073% (v/v) TFA. Analytical HPLC was carried out at a flow rate of 1 ml min^{-1}, semipreparative HPLC at 15–25 ml min^{-1}. Peak detection was performed by UV absorption at 220 nm. Semipreparative fractions were united from 7–14 separations and the solvent removed under vacuum to yield oily residues. These were treated with diethyl ether, which was subsequently removed to afford the products as powders. Their purity was monitored by analytical HPLC traces and ^{1}H NMR spectroscopy. HPLC conditions for complexes separated in this manner are listed in Table 3.

Mass spectral and NMR measurements

The FAB mass spectra were recorded on a Fisons VG Autospec instrument employing 3-nitrobenzyl alcohol as the matrix, ESI mass spectral measurements with Finnigen MAT double-focusing sector (MAT 95) and ion trap instruments. The 400 and 80 MHz NMR spectra were recorded at 298 K on respectively Bruker DRX 400 or WP 80 spectrometers using 5 mm tubes and D$_2$O as solvent. The chemical shift references were as follows: ^{1}H, sodium 3-(trimethylsilyl)tetradeuteriopropionate (δ 0.0); ^{195}Pt, saturated K$_2$[PtCl$_4$]–1 mol dm^{-3} NaCl (external) with δ −1628. pH* Values of solutions in NMR tubes were registered with a micro glass electrode (Hamilton spintrode 238100, length 180 mm).

References

1 R. F. Borch and M. E. Pleasants, *Proc. Natl. Acad. Sci. USA*, 1979, **76**, 6611.
2 C. M. Riley, L. A. Sternson, A. J. Repta and S. A. Slyter, *Anal. Biochem.*, 1983, **130**, 203.
3 J. Reedijk, *Chem. Commun.*, 1996, 801.
4 S. S. G. E. van Boom and J. Reedijk, *J. Chem. Soc., Chem. Commun.*, 1993, 1397.
5 K. J. Barnham, M. I. Djuran, P. del Socorro Murdoch and P. J. Sadler, *J. Chem. Soc., Chem. Commun.*, 1994, 721.
6 S. S. G. E. van Boom, Ph.D. Thesis, Leiden University, 1995.
7 J.-M. Teuben, S. S. G. E. van Boom and J. Reedijk, *J. Chem. Soc., Dalton Trans.*, 1997, 3979.
8 M. Iwanoto, S. Mukundan and L. G. Marzilli, *J. Am. Chem. Soc.*, 1994, **116**, 6233.
9 K. J. Barnham, Z. Guo and P. J. Sadler, *J. Chem. Soc., Dalton Trans.*, 1996, 2867.
10 K. J. Barnham, M. I. Djuran, P. del Socorro Murdoch, J. D. Radford and P. J. Sadler, *J. Chem. Soc., Dalton Trans.*, 1995, 3721.
11 A. F. M. Siebert and W. S. Sheldrick, *J. Chem. Soc., Dalton Trans.*, 1997, 385.
12 Z. Guo, T. W. Hambley, P. del Socorro Murdoch, P. J. Sadler and U. Frey, *J. Chem. Soc., Dalton Trans.*, 1997, 469.
13 T. Rau, R. Alfasser, A. Zahl and R. van Eldik, *Inorg. Chem.*, 1998, **37**, 4223.

14 C. D. W. Fröhling and W. S. Sheldrick, *Chem. Commun.*, 1997, 1737.

15 C. D. W. Fröhling and W. S. Sheldrick, *J. Chem. Soc., Dalton Trans.*, 1997, 4411.

16 T. G. Appleton, F. J. Pesch, M. Wienken, S. Menzer and B. Lippert, *Inorg. Chem.*, 1992, **31**, 4410.

17 J. P. Schneider and J. W. Kelly, *Chem. Rev.*, 1995, **95**, 2169.

18 M. R. Ghadiri and C. Choi, *J. Am. Chem. Soc.*, 1990, **112**, 1630.

19 F. H. Arnold and B. L. Haymore, *Science*, 1991, **252**, 1796.

20 N. L. Allinger, *J. Am. Chem. Soc.*, 1977, **99**, 8127.

21 A. F. M. Siebert, C. D. W. Fröhling and W. S. Sheldrick, *J. Chromatogr. A*, 1997, **761**, 115.

22 T. G. Appleton, J. W. Connor and J. R. Hall, *Inorg. Chem.*, 1988, **27**, 130.

23 K. Burger, in *Biocoordination Chemistry*, ed. K. Burger, Ellis Horwood, Chichester, 1990, p. 46.

24 A. W. Prestayko, in *Cisplatin, Current Status and New Developments*, eds. A. W. Prestayke, S. T. Crooke and S. K. Carter, Academic Press, London, 1980, p 2.

25 L. F. Heneghan and J. C. Bailar, jun., *J. Am. Chem. Soc.*, 1953, **75**, 1840; F. Basolo, J. C. Bailar, jun. and B. R. Tarr, *J. Am. Chem. Soc.*, 1950, **72**, 2433.